Environ. Sci. Technol. **2006**, *40,* 7890−7895

Collection of Ultrafine Diesel Particulate Matter (DPM) in Cylindrical Single-Stage Wet Electrostatic Precipitators

PHIRUN SAIYASITPANICH,[†] TIM C. KEENER,*[,†] MINGMING LU,[†] SOON-JAI KHANG,[‡] AND DOUGLAS E. EVANS[§]

Department of Civil and Environmental Engineering and Department of Chemical and Material Engineering, University of Cincinnati, Cincinnati, Ohio 45221, and Division of Applied Research and Technology, National Institute for Occupational Safety and Health, Centers for Disease Control and Prevention, Public Health Service, U.S. Department of Health and Human Services, 4676 Columbia Parkway MS-R3, Cincinnati, Ohio 45226

Long-term exposures to diesel particulate matter (DPM) emissions are linked to increasing adverse human health effects due to the potential association of DPM with carcinogenicity. Current diesel vehicular particulate emission regulations are based solely upon total mass concentration, albeit it is the submicrometer particles that are highly respirable and the most detrimental to human health. In this study, experiments were performed with a tubular single-stage wet electrostatic precipitator (wESP) to evaluate its performance for the removal of number-based DPM emissions. A nonroad diesel generator utilizing a low sulfur diesel fuel (500 ppm_w) operating under varying load conditions was used as a stationary DPM emission source. An electrical low-pressure impactor (ELPI) was used to quantify the number concentration distributions of diesel particles in the diluted exhaust gas at each tested condition. The wESP was evaluated with respect to different operational control parameters such as applied voltage, gas residence time, etc., to determine their effect on overall collection efficiency, as well as particle size dependent collection efficiency. The results show that the total DPM number concentrations in the untreated diesel exhaust are in the magnitude of $\sim 10^8/cm^3$ at all engine loads with the particle diameter modes between 20 and 40 nm. The measured collection efficiency of the wESP operating at 70 kV based on total particle numbers was 86% at 0 kW engine load and the efficiency decreased to 67% at 75 kW due to a decrease in gas residence time and an increase in particle concentrations. At a constant wESP voltage of 70 kV and at 75 kW engine load, the variation of gas residence time within the wESP from ∼0.1 to ∼0.4 s led to a substantial increase in the collection efficiency from 67% to 96%. In addition, collection efficiency was found to be directly related to the applied voltage, with increasing collection efficiency measured for increases in applied voltage. The collection efficiency based on particle size had a minimum for sizes between 20 and 50 nm, but at optimal wESP operating conditions it was possible to remove over 90% of all particle sizes. A comparison of measured and calculated collection efficiencies reveals that the measured values are significantly higher than the predicted values based on the well-known Deutsch equation.

Introduction

For many decades, diesel engines have served as a major power source in multipurpose applications such as transportation, excavation, and mining due to their excellent fuel economy and power. At the same engine size, the diesel engine today provides 35% better fuel economy and produces 25% more power (torque) than the equivalent displacement gasoline engine (*1*). In the United States, approximately 94% of all freight is moved by diesel engines (*2*). In Europe, diesel engines are being increasingly used to power passenger cars and are predicted to grow from 30% of the current light-duty diesel engine market to 50% by 2010 (*3*). While diesel engines clearly provide great benefits to our society, they are considered one of the largest sources for particulate emissions in urban air.

Diesel particulate matter (DPM) consists mainly of elemental carbon (EC), organic carbon (OC), and oxides. EC, the solid carbon (partially formed graphitic layers) portion of DPM, is a byproduct of incomplete combustion occurring in a locally fuel-rich region inside the engine combustion cylinder (*4*). OC is a complex mixture of unburned fuel, evaporated lube oil, and numerous soot-associated organic compounds including polycyclic aromatic hydrocarbons (PAHs) formed during combustion. According to the current DPM emission regulations, which are based only on the total mass, modern engines tend to emit lower total mass but are prone to produce higher concentrations of ultrafine particles (D_p < 100 nm) and nanoparticles (D_p < 50 nm) (*5*). Previous studies suggest that it is the number of small particles to which the individual is exposed that is the most detrimental to human health (*6*). Since DPM has typical size ranges between 5 nm and 1 μm with 90% of the particles less than 1.0 μm in aerodynamic diameter (*7*), there is a high probability for DPM to be inhaled and deposited in the respiratory tract (*8*), thus causing respiratory diseases and lung injury (*9*). For a given mass consisting of submicrometer particles, the number of particles will be much more than for an equivalent mass of larger particles, and results in a correspondingly larger available surface area compared with an equivalent mass of larger particles, thus allowing PAHs adsorption on their surfaces, with consequent airway deposition and contact, potentially resulting in an increase in lung cancer risk (*10*, *11*). While the advantages of diesel engines are clear, the impacts of DPM emissions are also evident. The potential of DPM emissions to be carcinogenic (*12*, *13*) has been a major driving force for both researchers and governmental agencies to seek promising and cost-effective control technologies.

Wet electrostatic precipitators (wESPs) have been used successfully for controlling SO_3 mist, which consists of submicrometer particles in power plant flue gas (*14*). The wESP operates in a three-step process: (1) charging the particles under nonuniform, very high electric field strength, (2) collecting the charged particles on the wet collecting

* Corresponding author phone: (513) 556-3676; fax: (513) 556-2599; e-mail: Tim.Keener@uc.edu.
[†] Department of Civil and Environmental Engineering, University of Cincinnati.
[‡] Department of Chemical and Material Engineering, University of Cincinnati.
[§] National Institute for Occupational Safety and Health.

10.1021/es060887k CCC: $33.50
Published on Web 10/25/2006

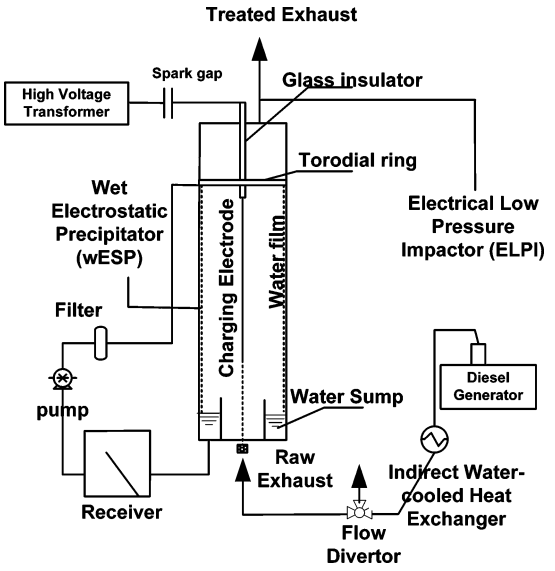

FIGURE 1. Schematic drawing of the experimental setup.

surface, and (3) cleaning the collected particles by washing the collecting electrode with liquid. This third step makes wESPs more advantageous over conventional dry ESPs when dealing with submicrometer particles or ultrafine particles.

At present, the available control technologies for diesel particulate emission control are diesel oxidation catalysts (DOCs) and diesel particulate filters (DPFs). The combination of DOCs and DPFs can provide 85−95% removal of mass-based DPM, HC, and CO. However, the limitations of these devices are their complexity in operation and regeneration, high energy consumption, backpressure, and high maintenance costs. In addition, the DOCs can further oxidize a portion of sulfur dioxide to sulfur trioxide, leading to formation of nuclei particles (10−80 nm) (*3*) after the DPFs when the exhaust gases cool. The goal of this study is to evaluate performance of a wet ESP as an alternative control for DPM emissions. The wESP offers the following advantages: moderate energy consumption, low maintenance requirements, simplicity in operation, and no interference in diesel engine operation.

Experimental Section

A nonroad diesel generator (Generac SD080) rated at 80 kW and 1800 rpm was used as a stationary DPM emission source (*15*). A load simulator (Merlin 100 manufactured by SIMPLX) was used to simulate loads by applying steady-state banks of heaters to the generator at 0, 25, 50, and 75 kW. Low sulfur diesel fuel (0.05% S) was used throughout these experiments.

Figure 1 shows the schematic diagram of the experimental setup. A single-stage, tube-type wESP made of carbon steel was designed to treat the diesel exhaust at the maximum flow rate of 500 actual m^3/hr with 0.1 s gas residence time under a very high turbulent flow regime (Re ∼16 000−66 000). The wESP (0.914 m long and 0.178 m i.d.) was equipped with a high-voltage stainless steel electrode (0.559 m long and 0.25 mm diameter), made taut by a weight. The charging electrode was energized with a DC voltage of negative polarity and controlled within a range of 0−72 kV by a Glassman high voltage transformer (WK125P5). An indirect water-cooled heat exchanger was used to cool the exhaust stream from ∼138−288 °C to ∼32−49 °C to prevent the evaporation of water and damage to Teflon and plastic connectors inside the wESP, but additionally to take advantage of the effects of flux force condensation on particle growth and agglomeration (*9*, *16*). This type of heat exchange could be easily accomplished on a commercial diesel engine by the use of an additional radiator. The collecting electrode was continuously irrigated by means of a water film, thus avoiding a breakdown of the electric field during flushing as occurs for spray irrigated systems. The water washing was a closed system and the flow rate was maintained between 2.27 and 3.18 L/min, which was found to efficiently and continuously generate a thin film of water on the wall of the wESP for washing the collected charged DPM particles and to prevent a sparking initiation between interelectrode spaces. The DPM laden water was then filtered and recirculated to the wESP.

An electrical low-pressure impactor (ELPI, Dekati) was used to quantify DPM number size distributions every second in the raw and treated diesel exhaust. The ELPI, a real-time cascade impactor (*17*), has operating principles based on a combination of the following: (1) diffusion charging of particles; (2) particle size classification based on aerodynamic diameter; (3) currents measured by electrometers at each electrically isolated stage; and (4) a conversion of measured current into a particle number concentration from known performance characteristics of the instrument (*18*). Oiled sintered metallic substrates were utilized at each stage, thereby reducing particle bounce and particle reentrainment.

The ELPI has been widely used in DPM measurement. It has been shown by various studies that the differential size distribution obtained by the ELPI is comparable with that of a scanning mobility particle sizer (SMPS), despite differences in the particle properties measured (electrical mobility versus aerodynamic diameter), while its accuracy in mass measurement is still under debate (*19*−*21*). Additionally, however, the ELPI does have some advantages of the SMPS, with a much greater temporal resolution and also a wider operating particle size range. In this study, only the number size distribution information (∼10−1000 nm) from the ELPI is utilized. For particles larger than approximately 1000 nm, the particle counts were found to be negligible (less than 0.01% of the smaller particles). Therefore only data below this diameter are reported in this paper.

Prior to entering the ELPI, the treated or untreated exhaust gas was diluted inside a mini-dilution chamber using dry, filtered ambient air so as to obtain appropriate particulate number concentrations for reliable ELPI measurement. The mini-dilution chamber is a 0.3-m long stainless-steel tube. The gas residence time inside the dilution chamber was about 2.5 s. The dilution ratio was adjustable from 0 to 100 by controlling the exhaust flow rate according to particulate concentrations under different engine loads. A portable, digital gas combustion analyzer (TESTO 350) was used to measure NO_x as an indicator of the dilution ratio. Collection efficiency of the wESP was determined by measuring particle number concentrations at the outlet of the wESP under the same conditions with and without energizing the discharge electrode. Relating the particulate concentration in the treated gas to that in the raw gas enabled the calculation of the collection efficiency.

Several particle charging and collection models have been proposed to predict the amount of charge on the particle and the removal efficiency of the charged particle inside the precipitator. Liu et al. (*22*, *23*), and Lawless (*24*) have presented numerical models taking into account the effects of diffusion, field, and combined charging, thus applicable for predicting electrical charge on the particles of all sizes. These models showed reasonable agreement with the experimental results. However, they need to be solved numerically and do not have analytical solutions. For practical work, it seems to be more reasonable to use analytical equations that describe charging processes continuously from small to larger particle sizes. In this paper, two particle charging models were used. The first particle charging model introduced by Cochet (*25*) for predicting charge on each particle is shown in eq 1. The model assumes that a particle of the same size attains an

equivalent maximum amount of charge (Q_p) for a charging time equal to infinity.

$$Q_p = \left\{\left(1 + \frac{2\lambda}{d_p}\right)^2 + \left(\frac{2}{1 + \frac{2\lambda}{D_p}}\right)\left(\frac{\epsilon_r - 1}{\epsilon_r + 2}\right)\right\}\pi\epsilon_0 D_p{}^2 E_{ps} \quad (1)$$

where λ is the mean free path of gas ions (m), D_p is the diameter of the particle (m), ϵ_r is the dielectric constant of the particle, ϵ_0 is the electrical permittivity of a vacuum, and E_{ps} is the pseudo-homogeneous electric field strength (V/m) as shown in eq 2.

$$E_{ps} = \frac{U}{R_{NE}} \quad (2)$$

where U is the applied voltage (V), and R_{NE} is the radius of the wESP (m). The dielectric constant (ϵ_r) of the dielectric particle normally lies between 1 and 10 (*26*). However, for the diesel particle generally comprised of complex chemical properties, it is very difficult to determine its dielectric value. Note that the dielectric constant of the diesel particle has not yet been reported elsewhere. Thus, in this paper this constant was determined by means of trial and error to optimize the model results.

The second particle charging model (*26*) shown in eq 3 was used to calculate the amount of charge on each particle during a time t according to Robinson (*27*) assuming that the gas residence time inside the wESP must be greater than 10−20 times the charging time constant (s). Equation 4 represents the charging time constant (τ).

$$Q_p = \left(\frac{3\epsilon_r}{\epsilon_r + 2}\right)\left(\frac{E_{ps}D_p{}^2}{4K_E}\right) + \frac{D_p kT}{2K_E e}\ln\left[1 + \frac{\pi K_E D_p \bar{c}_i e^2 N_i t}{2kT}\right] \quad (3)$$

$$\tau = \frac{4\epsilon_0}{N_i e Z_i} \quad (4)$$

where Q_p is the particle charge (C), $\bar{c}_i$ is the mean thermal speed of the ions (240 m/s at standard conditions), N_i is the concentration of ions (number/m^3), k is Boltzmann's constant (1.38×10^{-23} N·m/K), T is temperature (K), e is the electronic charge (1.6×10^{-19} C), K_E is a constant of proportionality (9×10^9 N·m^2/C^2), t is the gas residence time (s), and Z_i is the mobility of the ions (0.00015 m^2/V·s at standard conditions).

The first theoretical performance model for particle collection inside the precipitator has been suggested representatively by Deutsch (*28*). Deutsch assumed that a perfect mixing exists in the ESP (infinite diffusivity), thus creating a uniform particle concentration across the transverse section. However, in contrast to Deutsch's assumption, Cooperman (*29*), Leonard et al (*30*), Zhibin et al (*31*), and Riehle et al (*32*) attempted to develop finite diffusivity models for particle collection by integrating the convective-diffusion phenomena in wire-plate ESPs. Among those, Zhibin et al (*31*) also considered the effect of ionic wind on the diffusivity coefficient. For most cases, these models show ranges of collection efficiency between that of the Deutsch and laminar models for submicrometer particles. For cylindrical geometry, including the effects of the finite turbulent mixing and ionic wind would lead to a nonlinear partial differential equation that needs to be solved numerically. Thus, for the sake of simplicity, in this study only the laminar and Deutsch models were tested.

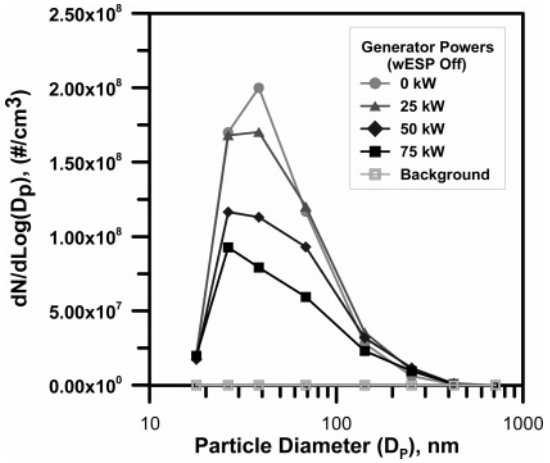

FIGURE 2. Dilution corrected DPM number size distributions measured during four loads (diluted sample temperature = ~4−7 °C; relative humidity = 64−79%; dilution ratio = 7−9).

The grade collection efficiency or fractional efficiency was calculated using eqs 5 and 6 (laminar model) and eq 7 (original Deutsch model).

$$\eta = D_e \text{ for } D_e < 1 \quad (5)$$

$$\eta = 1 \text{ for } D_e \geq 1 \quad (6)$$

$$\eta = 1 - \exp(-D_e) \quad (7)$$

where D_e is defined as

$$D_e = \frac{A_c \varpi_{th}}{Q} \quad (8)$$

where A_c is the effective collection area (m^2), Q is the exhaust volumetric flow rate (m^3/s), and ϖ_{th} is the theoretical migration velocity (m/s) given by eq 9 (*33*).

$$\varpi_{th} = \frac{Q_p E_{ps}}{3\pi\mu D_p} C_c \quad (9)$$

where C_c is the Cunningham correction factor and μ is the gas dynamic viscosity (kg/m·s).

Results and Discussion

DPM Size Distributions with Engine Loads. Figure 2 shows the DPM number size distributions measured during four engine load conditions with the wESP in the off mode. Three sample replicates (consisting of approximately 180 consecutive number size distribution measurements per sample replicate) were measured by the ELPI at each load condition (0, 25, 50, and 75 kW). The slipstream of the exhaust sample was drawn into a mini-dilution chamber where it was well mixed with dilution air (ambient air with the moisture content and background particles removed by silica gel and HEPA filter). The temperatures of the diluted gas were kept in the range of ~4−7 °C, relative humidity between 64 and 79%, and dilution ratios 7−9, respectively. The results show that the diesel particulate number size distributions had modes in the range of 30−40 nm for 0 and 25 kW and shifted toward lower sizes, i.e., 20−30 nm at the higher loads, 50 and 75 kW. In addition, it can be seen that the mode values decreased approximately 1- to 2-fold with increasing engine load. These observations are consistent with studies by Shi et al (*34*). For particles larger than ~250 nm, the DPM number concentrations show a reverse trend in which the particle number concentrations rise with increasing engine loads. The higher DPM number concentration at the lower load is believed to be primarily due to dilution, cooling, and amount of unburned fuel and lubricating oil in the exhaust sample (*9*). Diluting the engine exhaust with unheated, ambient air leads to a rapid reduction of the exhaust gas temperature from ~32−49 °C to ~4−7 °C, which triggers the homogeneous

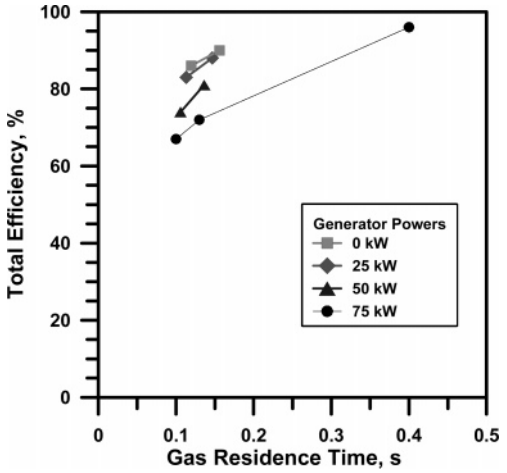

FIGURE 3. Wet ESP total collection efficiency versus gas residence time measured during four engine loads (diluted sample temperature = ~4−7 °C; relative humidity = 64−79%; dilution ratio = 7−32; wESP = 70 kV 3 mA, negative polarity, DC voltage).

nucleation process, and the nuclei particles formed may grow to larger sizes when heterogeneous condensation takes place. The magnitude of the gas-to-particle conversion strongly depends on the concentration of unburned fuel and oil present in the raw exhaust (*9*, *35*, *36*). As widely reported in previous studies (*4*, *9*, *34*, *37*), the amount of unburned fuel and oil is higher at the low engine load, thus leading to a higher formation of nuclei and accumulation mode particles during dilution and cooling processes, as observed in this study. The background particle number concentrations in the dilution air were also measured and found to be several orders of magnitudes lower than the DPM number concentrations.

Effects of Engine Loads and Gas Residence Time on Collection Efficiency of wESP. Figure 3 presents the collection efficiency of the wESP on total DPM number concentrations as a function of the engine loads and gas residence time. The DPM size distributions were measured by the same method as described in the preceding section. The sampling conditions were kept the same except that the dilution ratio was controlled in the range of 7−32. The wESP was operated at a constant voltage of 70 kV corresponding to a corona current of 3 mA in all tests. A different amount of exhaust gas was fed into the wESP to account for different gas residence times of ~0.1−0.16 s (at 0, 25, and 50 kW) and ~0.1−0.4 s (at 75 kW). The gas residence time was slightly different for each engine load, albeit the ratios of the exhaust flow fed into the wESP to the total exhaust emitted from the engine were kept constant (100% and 77% for 0, 25, and 50 kW, and 100%, 77%, and 25% for 75 kW) due to the fact that the exhaust flowrate is slightly reduced with decreasing engine loads (*38*).

The results indicate that the collection efficiencies were strongly influenced by the gas residence time and also the engine load. At the 100% exhaust flowrate corresponding to a gas residence time of ~0.1 s, the collection efficiency increased from 67% to 86% when the engine power was reduced from 75 to 0 kW, respectively. The effect of increasing engine power, which in turn led to a change in DPM characteristics, was more pronounced than that of the residence times at a given condition. It is believed that the wESP may efficiently remove the unburned fuel and lubricating oil (higher concentrations at lower engine loads) from the diesel exhaust, thus suppressing the gas-to-particle conversion mechanism inside the mini-dilution chamber. Research is currently underway to verify this assumption. At higher gas residence times proportional to higher specific

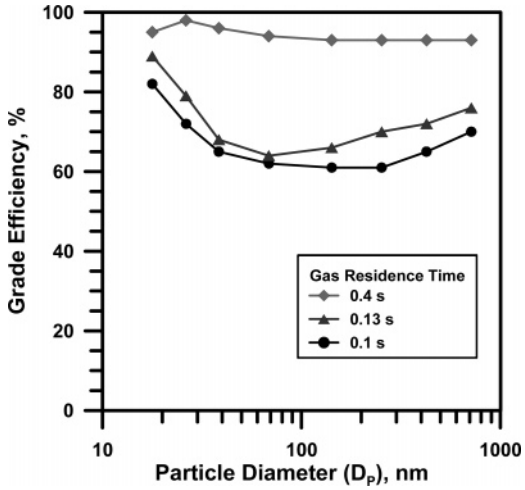

FIGURE 4. Wet ESP grade collection efficiency versus particle sizes measured at a 75-kW engine load with different gas residence time (diluted sample temperature = ~4−7 °C; relative humidity = 42−68%; dilution ratio = 7−32; wESP = 70 kV 3 mA, negative polarity, DC voltage).

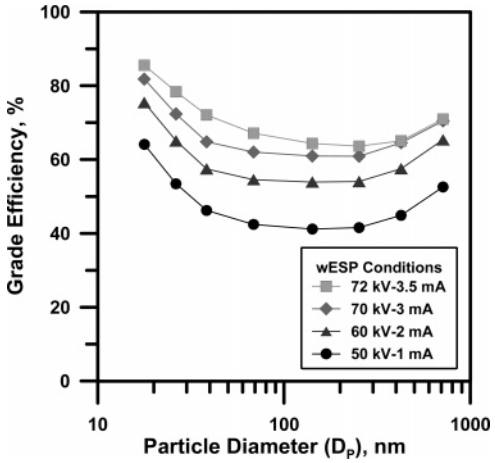

FIGURE 5. Wet ESP grade collection efficiency versus particle sizes measured at a 75-kW engine load with different corona powers (diluted sample temperature = ~4−7 °C; relative humidity = 42−68%; dilution ratio = 7−32; negative polarity, DC voltage).

collection area (SCA), the removal efficiency increased regardless of the engine load. Figure 4 indicates that, at the 75-kW engine load, the wESP was capable of removing ~96% DPM based on total number concentrations equivalent to more than 93% grade efficiency for particles of each size at gas residence time of ~0.4 s.

Effects of wESP Power Levels on Collection Efficiency. Figure 5 shows the variations of the fractional efficiency as a function of DPM diameters for various values of the charging voltages. As expected, there is a strong effect of the charging voltages on collection efficiency. At increasing voltage, the corona current increased, which led to an increasing ion density, thus enhancing the particle charging and collection processes inside the wESP (higher particle migration velocity). The wESP efficiency had a minimum for particle sizes between 80 and 250 nm. In this size range, the particles possess a minimum electrical mobility compared with smaller or larger particles due to the combined effects of diffusion and field charging mechanisms. Hence, the electrical mobility cannot compensate the relatively lower level of charge and lead to lower migration velocity of the particles in this size range. More detailed explanations of this effect are widely published elsewhere (*26*). The wESP performance at 72 kV

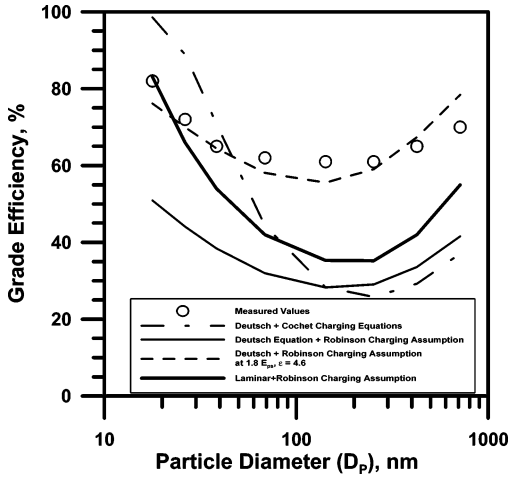

FIGURE 6. Comparison of measured and predicted collection efficiency (Deutsch equation in association with Cochet equations and Robinson charging assumption; 75 kW engine load, 100% exhaust flow rate (0.138 m³/s); wESP = 70 kV 3 mA, negative polarity, DC voltage).

may have been affected by intermittent sparking occurring between the interelectrode spaces during the measurement, which tends to deteriorate the collection efficiency of the wESP.

Comparison of Measured and Calculated Collection Efficiency. Figure 6 presents a comparison between the measured and calculated collection efficiency of the wESP. The measured values are higher than those predicted using the Deutsch and Cochet charging equations, eqs 7 and 1 (*39*), for particle diameters between 40 nm and 1 μm. This result is consistent, however, with studies by Riehle et al (*32*) and Wadenpohl et al (*40*). Moreover, the measured values are substantially higher than those predicted using the Deutsch equation with the Robinson charging assumption, eqs 7 and 3 (*41*), for particles of all sizes. The predicted values using the laminar model with Robinson assumption showed better agreement with the measured values for particle diameters less than 40 nm. The Deutsch and Cochet charging equations assume the charging time to be infinity (*39*), which most likely leads to an overprediction of the collection efficiency for particles smaller than 40 nm. This assumption may not be realistic in this experiment where the residence time is 0.1 s. Evidently, the Deutsch equation in collaboration with the Cochet charging equation and the Robinson charging assumption is not accurate in describing the particle collection effectively. As a result, the simplified charging and collection models may not be adequate in this case. The use of numerical models to predict the particle charge may lead to higher particle charge quantity and therefore result in higher collection efficiency. Furthermore, it may be anticipated that the effect of an inhomogeneous electric field distribution may lead to a distinct increase in collection efficiency of the wESP for the ultrafine particles (*42*). Previous studies have reported that a numerical particle tracking model (PTM) incorporating a computational fluid dynamic (CFD) flow simulation, taking into account the effect of finite turbulent diffusivity and inhomogeneous electric field strength, showed better agreement between predicted and measured results (*43*). Previous studies have also shown that the effect of a secondary turbulent flow induced by the corona wind may also improve the collection efficiency when the electrohydrodynamic number (N_{EHD}) is less than 1 (*31*).

Sensitivity of Electric Field Strength and DPM Dielectric Constant on Calculated Collection Efficiency. To observe the effect of the electrical field strength on the collection efficiency predicted by Deutsch model with Robinson charging assumption, the sensitivity of the electric field was evaluated by varying the values of electric field strength in those equations. By minimizing the sum of squares of the difference between the measured values and the calculated values obtained from the equation using different electric field strengths, the optimized electric field strength was found equal to 1.8 times the pseudo-homogeneous electric field strength (E_{ps}) initially used in the calculations. In reality, the space charge density induced by charged particles and ions influences the electric field strength (E) inside the wESP and, in some cases, may lead to higher average electric field strength than E_{ps} (*41*). Note that the value of 1.8 found in this study is not universal but purely depending on several parameters such as wESP geometry and operating conditions. This study only attempted to show how sensitive the electric field strength is to the particle collection efficiency. As discussed before, information for the dielectric constant (ϵ_r) for the DPM is still missing. Thus, the sensitivity of the dielectric constant was also evaluated and found to be optimized at a value of 4.6. As illustrated in Figure 6, the dashed line represents the predicted values obtained from the use of the Deutsch equation and Robinson assumption with the optimal values of E and ϵ_r. These results illustrate the importance in determining the values of the electric field strength in attempting to predict collection efficiency in the wESP.

Acknowledgments

Financial support from the National Institute for Occupational Safety and Health is gratefully acknowledged. The findings and conclusions in this report are those of the authors and do not necessarily represent the views of the National Institute for Occupational Safety and Health. Mention of a company name or product does not constitute endorsement by the Centers for Disease Control and Prevention.

Literature Cited

(1) McManus, W. Diesel Advantages; Hybrid and Diesel Markets. HybridCARS.com. www.hybridcars.com/hybrid-versus-diesel.html (accessed 2005).
(2) Diesel Particulate Matter Emission Reduction Measures. Washington Statue University Extension Energy Program. www.energy.wsu.edu/ftp-ep/pubs/renewables/DieselPMEmissionReductionMeasures.pdf (accessed 2005).
(3) Walker, A. P. Controlling Particulate Emissions from Diesel Vehicles. *Topics Catal.* **2004**, *28*, 165−170.
(4) Liu, Z.; Lu, M.; Birch, M. E.; Keener, T. C.; Khang, S. J; Liang, F. Variations of the Particulate Carbon Distribution from a Nonroad Diesel Generator. *Environ. Sci. Technol.* **2005**, *39*, 7840−7844.
(5) Bagley, S. T. Characterization of Fuel and After treatment Device Effects on Diesel Emissions; Health Effects Institute Research Report No. 76; HEI: Boston, MA, 1996; p 88.
(6) Donaldson, K.; Li, X. Y.; MacNee, W. Ultrafine (nanometer) Particle Mediated Lung Injury. *J. Aerosol Sci.* **1998**, *29* (5), 553−560.
(7) Kittelson, D.; Watts, W.; Ramachandran, G.; Paulsen, D.; Kreager, C. *Measurement of Diesel Aerosol Exposure: A Feasibility Study*; Research Directions to Improve Estimates of Human Exposure and Risk from Diesel Exhaust, Special Report of the Institute's Diesel Epidemiology Working Group; Health Effects Institute: Boston, MA, 2002.
(8) International Agency for Research on Cancer. *IARC Monographs on the Evaluation of Carcinogenic Risks to Humans: Diesel and Gasoline Engine Exhausts and Some Nitroarenes*; No. 46; IARC: Lyon, France, 1989,; p 458.
(9) Ning, Z.; Cheung, C. S.; Liu, S. X. Experimental Investigation of the Effect of Exhaust Gas Cooling on Diesel Particulate. *J. Aerosol Sci.* **2004**, *35*, 333−345.
(10) Lloyd, A. C.; Cackette, T. A. Diesel Engines: Environmental Impact and Control. *J. Air Waste Manage. Assoc.* **2001**, *51*, 809−847.
(11) Enya, T.; Suzuki, H.; Watanabe, T.; Hirayama, T.; Hisamatsu, Y. 3-Nitrobenzanthrone, A Powerful Bacterial Mutagen and Sus-

pected Human Carcinogen Found in Diesel Exhaust and Airborne Particulates. *Environ. Sci. Technol.* **1997**, *31* (10), 2772−2775.
(12) U.S. Department of Health and Human Services, Public Health Service, Centers for Disease Control, National Institute for Occupational Safety and Health, DHHS. *Carcinogenic Effects of Exposure to Diesel Exhaust*; Current Intelligence Bulletin No. 50, Publication No. 88-116; NIOSH: Cincinnati, OH, 1998.
(13) U.S. Environmental Protection Agency, National Center for Environmental Assessment. *Health Assessment Document for Diesel Emission*; Review Draft EPA/600/8-90/057E; U.S. EPA: Washington, DC, 2000.
(14) Bayless, D. J.; Shi, L.; Kremer, G.; Stuart, B. J. Membrane-Based Wet Electrostatic Precipitation. *J. Air Waste Manage. Assoc.* **2005**, *55*, 784−791.
(15) *Manual of the Generac Diesel Generator (Model SD080)*; Tri-State Generator, Cincinnati, OH.
(16) Altman, R.; Buckley, W.; Ray, I. Wet Electrostatic Precipitation: Demonstrating Promise for Fine Particulate Control. *Power Eng.* **2001**, *105* (1), 37−44.
(17) Keskinen, J.; Pietarinen, K.; Lehtimäki. Electrical low-pressure imapctor. *J. Aerosol. Sci.* **1992**, *23* (4), 353−360.
(18) Marjamäki, M.; Keskinen, J.; Chen, D. R.; Pui, D. Y. H. Performance evaluation of the electrical low-pressure impactor (ELPI). *J. Aerosol Sci.* **2000**, *31* (2), 249−261.
(19) Kinsey, J. S.; Mitchell, W. A.; Squier, W. C.; Linna, K.; King, F. G.; Logan, R.; Dong, Y. J.; Thompson, G. J.; Clark, N. N. Evaluation of Methods for the Determination of Diesel-Generated Fine Particulate Matter: Physical Characterization Results. *J. Aerosol Sci.* **2006**, *37* (1), 63−87.
(20) Gulijk, V. C.; Marijnissen, J. C. M.; Makkee, M.; Moulijn, J. A.; Schmidt-Ott, A. Measuring Diesel Soot with a Scanning Mobility Particle Sizer and an Electrical Low-Pressure Impactor: Performance Assessment with a Model for Fractal-Like Agglomerates. *J. Aerosol Sci.* **2004,** *35* (5), 633−655.
(21) Maricq, M. M.; Podsiadlik, D. H.; Chase, R. E. Size Distributions of Motor Vehicle Exhaust PM: A Comparison between ELPI and SMPS Measurements. *Aerosol Sci. Technol.* **2000**, *33* (3), 239−260.
(22) Liu, B. Y. H.; Yeh, H. C. On the Theory of Charging of Aerosol Particles in an Electric Field. *J. Appl. Phys.* **1968**, *39* (3), 1396−1402.
(23) Liu, B. Y. H.; Kapadia, A. Combined Field and Diffusion Charging of Aerosol Particles in the Continuum Regime. *J. Aerosol Sci.* **1978**, *9*, 227−242.
(24) Lawless, P. A. Particle Charging Bounds, Symmetry Relations, and an Analytic Charging Rate Model for the Continuum Regime. *J. Aerosol Sci.* **1996**, *9*, 191−215.
(25) Cochet, R. Lois Charge des Fines Particules (Submicroniques) Etudes Théoretiques-Controles Récents Spectre de Particules. Coll. Int. la Physique des Forces Electrostatiques et Leurs Application. *Cent. Nat. Rech. Sci.* **1961**, *102*, 331−338.
(26) Hinds, W. C. *Aerosol Technology: Properties, Behavior, and Measurement of Airborne Particles*, 2nd ed.; John Wiley & Sons, Inc.: New York, 1999; pp 323−331.
(27) Robinson, M. *Electrostatic Precipitation: Air Pollution Control Part I*; Interscience Publishers, John Wiley & Son, Inc.:, New York, 1971; p 262.
(28) Deutsch, W. Bewegung und Ladung der Elektrizitatstrager im Zylinderkondensator. *Annal. Phys.* **1922**, *68*, 335−344.
(29) Cooperman, P. A New Theory of Precipitator Efficiency. *Atmos. Environ.* **1971**, *5*, 541−551.
(30) Leonard, G.; Mitchner, M.; Self, S. A. Particle Transport in Electrostatic Precipitators. *Atmos. Environ.* **1980**, *14*, 1289−1299.
(31) Zhibin, Z.; Guoquan, Z. Investigation of the Collection Efficiency of an Electrostatic Precipitator with Turbulent Effects. *Aerosol Sci. Technol.* **1994**, *20*, 169−176.
(32) Riehle, C.; Löffler, F. Grade Efficiency and Eddy Diffusivity Models. *J. Electrostat.* **1995**, *34*, 401−413.
(33) Oglesby, S. *A Manual of Electrostatic Precipitator Technology-Part 1- Fundamentals*; Southern Research Institute: Birmingham, AL, 1970; pp 69−95.
(34) Shi, J. P.; Harrison, R. M.; Brear, F. Particle Size Distribution from a Modern Heavy Duty Diesel Engine. *Sci. Total Environ.* **1999**, *235*, 305−317.
(35) Kittelson, D. B. Engines and Nanoparticulates: A Review. *J. Aerosol Sci.* **1998**, *29*, 575−588.
(36) Kim, D.; Gautam, M.; Gera, D. Parametric Studies on the Formation of Diesel Particulate Matter via Nucleation and Coagulation Modes. *J. Aerosol Sci.* **2002**, *33*, 1609−1621.
(37) Wong, C. P.; Chan, T. L.; Leung, C. W. Characterization of Diesel Exhaust Particle Number and Size Distributions Using Mini-Dilution Tunnel and Ejector-Diluter Measurement Techniques. *Atmos. Environ.* **2003**, *37*, 4435−4446.
(38) Saiyasitpanich, P.; Lu, M.; Keener, T. C.; Khang, S. J.; Liang, F. The Effect of Diesel Fuel Sulfur Content on Particulate Matter Emissions for a Nonroad Diesel Generator. *J. Air Waste Manage. Assoc.* **2005**, *55*, 993−998.
(39) Dumitran, L. M.; Atten, P.; Blanchard, D.; Notingher, P. Drift Velocity of Fine Particles Estimated from Fractional Efficiency Measurements in a Laboratory-Scaled Electrostatic Precipitator. *IEEE Trans. Ind. Appl.* **2002**, *38*, 852−857.
(40) Wadenpohl, C.; Peukert, W. Collection of Submicron Particles in Wet Electrostatic Precipitators. PARTEC 98, 4th European Symposium Separation of Particles from Gases, Nürnberg/Germany, 10−12. March 1998.
(41) Crawford, M. *Air Pollution Control Theory*; McGraw-Hill: New York, 1976; pp 298−358.
(42) Peukert, W.; Wadenpohl, C. Industrial Separation of Fine Particles with Difficult Dust Properties. *Powder Technol.* **2001**, *118*, 136−148.
(43) Parker, K. R. *Applied Electrostatic Precipitation*, 1st ed.; Blackie Academic & Professional: New York, 1997; pp 25−87.

Received for review April 12, 2006. Revised manuscript received September 7, 2006. Accepted September 18, 2006.

ES060887K